Journal of Physics:
Conference Series

PAPER • **OPEN ACCESS**

Potential Benefits of Including Motion Sickness Predictions in an Offshore Wind Operational Planning Tool

To cite this article: Jesse Bloothoofd *et al* 2025 *J. Phys.: Conf. Ser.* **3131** 012046

Journal of Physics: Conference Series **3131** (2025) 012046 doi:10.1088/1742-6596/3131/1/012046

Potential Benefits of Including Motion Sickness Predictions in an Offshore Wind Operational Planning Tool

Jesse Bloothoofd[1*], Jan Souman[2], Johan Peeringa[1], Jelte Bos[2], Harald van der Mijle Meijer[1], Wouter Engels[1]

[1] Wind Energy, TNO, Petten, Netherlands
[2] Integrated Vehicle Safety, TNO, Helmond, Netherlands

[*]E-mail: jesse.bloothoofd@tno.nl

Abstract. The challenges of offshore wind energy maintenance, particularly in addressing motion sickness among technicians, have implications for both safety and operations. Current methodologies often rely on simplistic metrics such as Motion Sickness Incidence (MSI), which fail to capture symptoms preceding emesis. This study introduces a novel motion sickness model based on the Motion Illness Symptoms Classification Scale (MISC), which accounts for a broader spectrum of symptoms and integrates three-dimensional linear accelerations. By incorporating motion sickness predictions into decision-making processes, this approach enables more informed planning strategies, optimizing technician well-being and operational efficiency. Through case studies evaluating various scenarios, including vessel speed adjustments, route deviations, and technician rest periods, the model offers insights into mitigating motion sickness and improving offshore wind operations.

1. Introduction

Offshore wind energy has emerged as an important energy source in the global transition toward sustainable energy. With advancements in technology and cost reductions, the sector has seen exponential growth, increasing its global installed capacity by almost a factor of 15 between 2012-2023 [1]. To accommodate this increasing growth, various challenges during the operations and maintenance (O&M) phase will have to be addressed.

Accessing offshore wind farms for operations and maintenance (O&M) is challenging due to the motion of crew transfer vessels (CTVs) caused by wind and waves. This motion can lead to motion sickness among technicians and crew, resulting in reduced well-being, safety risks, and decreased productivity. Studies, such as Bos [2], have shown that task failures increase with sickness. Seasickness can persist even after exposure to motions and may worsen in different motion environments, like wind turbines. Severe illness may even require the CTV to return to shore, impacting operational expenditures (OPEX). Consequently, wind farm operators should consider seasickness risks in their decision-making to ensure safety and cost efficiency.

Several studies have examined the relationship between vessel motion and motion sickness in offshore wind operations, highlighting key advancements in decision-making tools and methodologies. The SPOWTT project [3, 4] developed a novel model to predict sea sickness based on vessel acceleration in all three axes at specific frequencies. It was integrated into Despatch [5],

an O&M decision support tool developed by TNO, to enable vessel speed adjustments and prevent sickness beyond a certain threshold. Another study [6] introduced a numerical tool that evaluates vessel motion-based measures of workability by simulating the entire O&M process, providing a more reliable assessment of weather windows compared to traditional metocean thresholds. Additionally, [7] employed Motion Sickness Incidence (*MSI*)—the percentage of passengers vomiting after two hours of motion exposure—as a parameter for determining vessel workability, allowing thrust adjustments to keep *MSI* below a 25% threshold, improving workability at the cost of longer transit times. Building on [4], [8] validated these tools through onboard vessel measurements, refining hydrodynamic response validations, enhancing weather forecast error corrections, and improving decision-making dashboard functionality.

Current studies on motion sickness in offshore wind operations often use Motion Sickness Incidence (MSI) to estimate vomiting probability, overlooking other symptoms like fatigue, dizziness, lack of focus, and nausea that affect technicians' performance and well-being. Additionally, mitigation options in these studies are limited to reducing vessel speed and rerouting, without exploring alternatives like recovery breaks at wind turbines.

This study aims to apply the Motion Illness Symptoms Classification (MISC) scale to offshore wind applications, predicting a range of symptoms and accounting for linear accelerations in three axes (x, y, z). Case studies will demonstrate integrating this model with vessel motion models for O&M planning tools like Despatch [5]. Scenarios will include altering vessel speed, using alternative routes, and taking breaks at wind turbines for recovery. The study will also examine the effects of passenger locations on the vessel and the sensitivity of different populations to motion sickness.

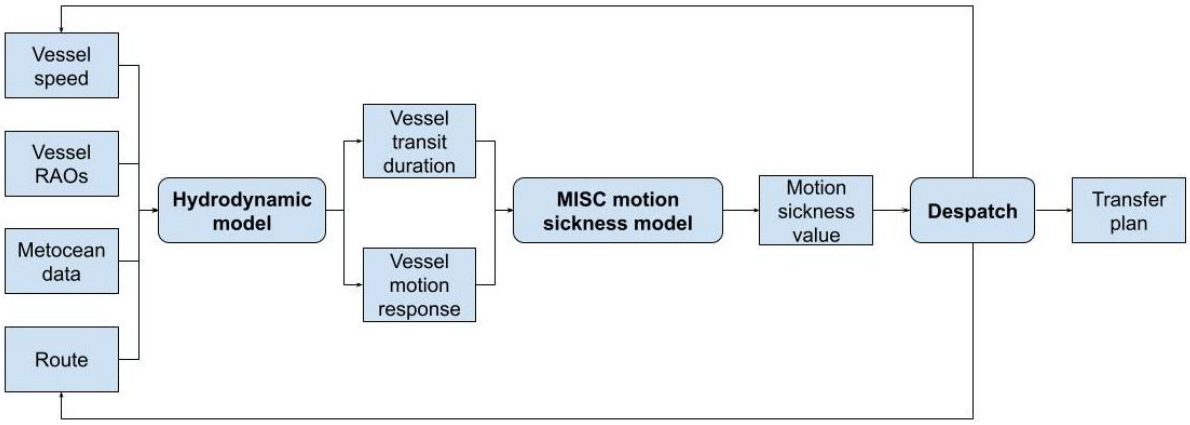

Figure 1. Process overview of the dependencies between hydrodynamic motion model, the motion sickness model, and Despatch.

2. Methodology

The process overview and interdependencies among the vessel motion model, motion sickness model, and the daily O&M planning tool (Despatch) are illustrated in Figure 1. While the aim is to fully integrate these models into a unified framework, the current study excludes direct integration with Despatch. Instead, the consequences of changed planning in this work are evaluated with the vessel motion and motion sickness models only.

The following sections provide a detailed description of each model and tool, outlining their functionalities and interconnections.

2.1 Despatch

Despatch is a software tool designed to optimize the operational planning of offshore wind farm maintenance activities [5]. It is based on the UWiSE engine [9], a discrete event simulation tool developed by TNO for modeling offshore wind logistics. Despatch aims to address the complex management of maintenance activities as wind farms become larger. Currently, most wind farm operators schedule these operations manually, which becomes increasingly difficult with a larger number of tasks. Instead, Despatch automates this process using optimization techniques.

Despatch employs a combination of simulation and optimization techniques to generate efficient daily maintenance plans (Transfer Plans) based on a list of open tasks (Work Orders), which include details such as turbine numbers, wind speed restrictions, and required man hours. These plans assign tasks to technician teams based on their skill sets and allocate vessels for transport. A genetic algorithm (GA), a metaheuristic optimization algorithm, enables Despatch to efficiently explore numerous transfer plan possibilities by mimicking natural evolution through selection, crossover, and mutation. This approach allows the tool to consider factors like technician availability, weather accessibility, and task durations, identifying the most efficient plan. The UWiSE simulation engine evaluates each plan by replicating real-world conditions, including technician shifts, weather impacts, vessel transit, and task completion, ultimately aiding in selecting plans that maximize energy production or minimize losses.

2.2 Vessel motions model

The accelerations experienced by crew members during transit, waiting, or in the turbine can cause motion sickness. These accelerations, influenced by the ship's motion and location, are crucial inputs for the motion sickness model. The ship's motion depends on the sea state and the ship's response, as explained by Journée and Massie [10].

The sea state is modeled using a JONSWAP wave spectrum, and accelerations are provided by MARIN as Response Amplitude Operators (RAO). For a given wave direction, vessel speed, and position on the ship, an RAO gives the acceleration amplitude and corresponding phases for a range of wave frequencies (ω_0).

For a vessel with forward speed V, the encounter frequency ω_e differs from the wave frequency ω_0 due to a Doppler shift:

$$\omega_e = \omega_0 - \frac{\omega_0^2}{g} V \cos\mu$$

Where μ is the wave direction. The wave energy shifts to higher frequencies in the encounter frequency domain. The acceleration response spectrum in the encounter frequency domain is calculated as:

$$S_a(\omega_e) = |a(\omega_e)|^2 S_\xi(\omega_e)$$

where S_a is the acceleration response spectrum, a is the acceleration amplitude, and S_ξ is the JONSWAP wave spectrum. Currently, the power spectral density of accelerations is generated only for incoming waves, with future projects addressing following seas.

2.3 Motion sickness model

ISO standard 2631-1:1997 predicts motion sickness aboard large ships using the Motion Sickness Dose Value (MSDV), which is based on time-integrated, frequency-weighted vertical acceleration. The standard, derived from post-WWII studies [11, 12], shows peak sensitivity around 0.17 Hz and estimates the percentage of people expected to vomit (MSI) using the equation:

$$MSI = k * MSDV_z$$

for an average population. If the power spectrum of vertical ship motion is constant over time, the $MSDV_z$ increases proportionally with the square root of time during motion exposure.

While effective for predicting vomiting from vertical motion, the model has limitations for crew transfer vessels and maintenance planning. It does not account for other symptoms like drowsiness, dizziness, or nausea, which affect performance and well-being [2]. The model also only considers vertical acceleration, ignoring significant horizontal accelerations experienced on smaller vessels like CTVs, whereas previous research suggests that horizontal accelerations also contribute to motion sickness [13, 14, 15]. Additionally, it does not factor in individual susceptibility variations such as age and gender. Therefore, ISO 2631-1 is limited in preventing or reducing motion sickness effects during crew transports by modifying vessel velocity or course.

To address the limitations of the ISO 2631-1 model, TNO developed an extended motion sickness model that considers 3 degrees of freedom acceleration (longitudinal, lateral, and vertical) and predicts the proportion of passengers experiencing various degrees of motion sickness. This model uses the Motion Illness Symptoms Classification (MISC) scale, which rates motion sickness from 0 (no symptoms) to 10 (emesis), with intermediate values indicating symptoms like nausea, drowsiness, and headache [16, 17].

The new model applies a modified frequency weighting function to the acceleration input, reflecting increased sensitivity for frequencies above 0.17 Hz. It combines the MSDVs for the three motion axes by weighting each axis's impact on motion sickness and computing the Euclidean distance. This 3 degrees of freedom MSDV is then used in a probability function to predict the likelihood of motion sickness symptoms above a certain MISC value.

The model also accounts for individual susceptibility to motion sickness, considering factors like age, gender, and viewing conditions. Validated for lower accelerations typically encountered in land-based vehicles (up to 4 m/s^2), its accuracy beyond this range remains uncertain.

The orientations and frame of references used in the motion sickness model follow a similar definition as the SPOWTT project [4].

3. Results and discussion

A series of scenarios are presented to evaluate the impacts of seasickness on personnel and to demonstrate the combined hydrodynamic and motion sickness model. The scope of these scenarios is inherently constrained by the hydrodynamic model employed, which accounts only for incoming wave conditions into the bow of the ship. This limitation excludes scenarios involving waves approaching from the stern. Consequently, the scenarios are specific to head-sea conditions.

The scenarios include two wind farms. The first is Offshore Windpark Egmond aan Zee (OWEZ), featuring 36 Vestas 3MW V-90 wind turbines located approximately 18 km offshore. The second is Princess Amalia Wind Park (PAWP), with 60 Vestas 2MW V-90 turbines located 23 km from shore. Various operational scenarios are analyzed, including the effects of different positions on the vessel and the impact of detours as alternative routes. Vessel speed variations were evaluated to understand their influence on motion-induced discomfort, particularly motion sickness. Additionally, a range of wave conditions is simulated to examine their effect on seasickness prevalence. Finally, the impact of the susceptibility of different population percentages to seasickness is evaluated.

Scenario	Start point(s) (UTM)	End point(s) (UTM)	Vessel speed (knots)	Wave height Hs (m)	Wave period Tp (s)	Wave direction	Wind farm
Scenario 1	(604660, 5814085)*	(597183, 5826381)*	25	1.5, 1.0	5.5, 5.0	North	OWEZ
Scenario 2	(600000, 5800000)	(590000, 5810000)	15, 20, 25	1.5	5.5	North	N/A
Scenario 3	(606732, 5813594); … (584022, 5829007)	(585371, 5827027); … (580531, 5827405)	25	1.5	5.5	North	PAWP

*Table 1: Overview of the start and end coordinates of the scenarios in UTM coordinates for UTM zone 31U, the vessel speed, the wave height, wave period, wave directions, and the wind farms. *For the deviated routes, an additional start- and end-point were used.*

Three specific scenarios (Table 1 and Figure 2) are selected to assess the effects of varying conditions during vessel transits. Each scenario involves a Crew Transfer Vessel (CTV) with a catamaran-shaped hull, used for conducting a series of transits. Each transit is divided into segments with specific start and end points, defined using the Universal Transverse Mercator (UTM) coordinate system.

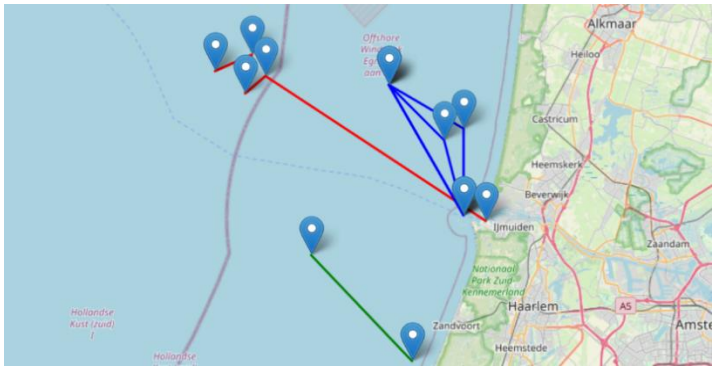

Figure 2. Vessel routes for the three scenarios visualized on a map. Markers indicate waypoints, while line segments represent the transit paths. Scenario 1 is shown in blue, Scenario 2 in green, and Scenario 3 in red.

Scenario 1 involves a transit from the Port of IJmuiden to a single wind turbine. Initially, the power spectrums are analyzed to understand the energy distribution across different frequencies. Subsequently, the impact of varying positions on the vessel is evaluated, followed by an assessment of the crew's differing susceptibilities to seasickness. Finally, the scenario explores the effects of calmer sea conditions on the transit.

Scenario 2 evaluates the effects of varying vessel speeds over a specific segment. This study's RAO data features a relative incoming wave angle resolution of 5 degrees at 25 knots. However, for speeds below 25 knots, the resolution becomes worse as a result of 15-degree intervals. Incoming wave angles are rounded to the nearest resolution step, potentially introducing greater rounding effects at speeds below 25 knots compared to 25 knots. To mitigate this, Scenario 2 selects start and end points that ensure an incoming wave angle alignment that eliminates the need for rounding, regardless of the vessel's speed. In contrast, it could not be guaranteed that this rounding would not occur in Scenario 1.

Scenario 3 examines a transit involving sequential visits to multiple wind turbines. A brief pause is introduced at the first turbine, and its impact on motion sickness among the crew is evaluated.

Scenario 1

Figure 3 illustrates the power spectra and Root Mean Square (RMS) values for scenario 1. The power spectra show the accelerations in three directions across multiple positions on the boat, with the RMS values given for each location. The analysis reveals that most energy is in the ship's

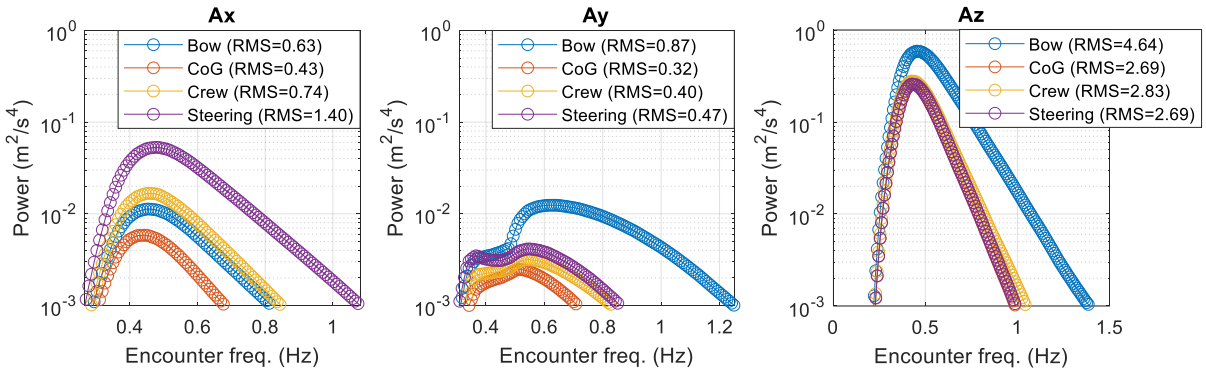

Figure 3. Scenario 1 - Power spectrums and RMS values for the bow, centre of gravity (CoG), crew, and steering locations for the accelerations in the x-direction (left), y-direction (middle), and z-direction (right).

heave motion (z-direction). Notably, the bow exhibits the highest energy levels across all positions on the boat. This observation aligns with expectations, as the bow's location, being relatively far from the boat's center, is amplified by the tangential and centripetal accelerations of rotational motion.

The motion sickness results are expressed as the probability that an individual experiences symptoms greater than a given MISC value, based on their susceptibility level. Susceptibility represents an individual's sensitivity to motion sickness, based on past experiences (within the range [0, 1]). Figure 4 illustrates the motion sickness MISC values for four positions on the vessel, calculated for a susceptibility of 0.25. This corresponds to the 25% of individuals least sensitive to motion sickness. This threshold is intentionally selected because individuals susceptible to motion sickness are deemed unlikely to continue long-term careers in offshore environments.

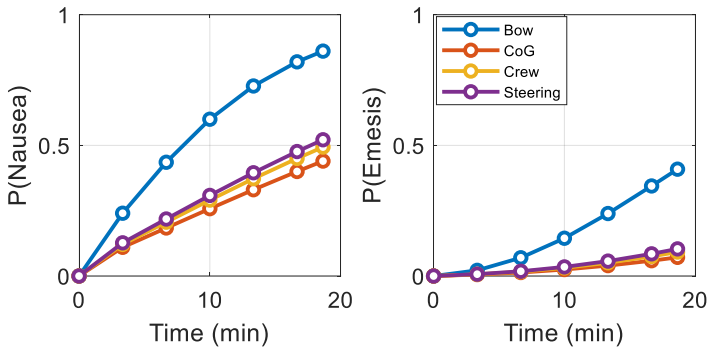

Figure 4. Scenario 1 - MISC results for P(MISC > 5) (left) and P(MISC>9) (right) for various positions on the vessel.

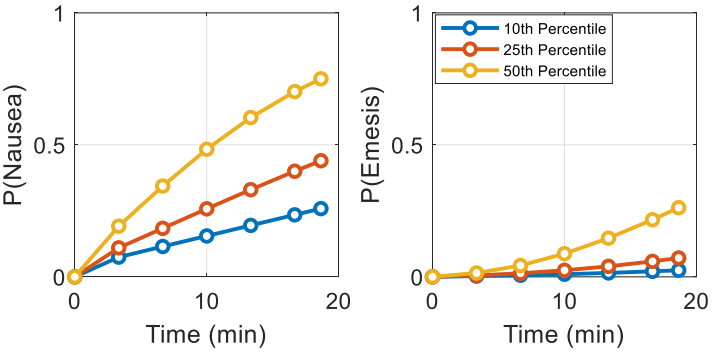

Figure 5. Scenario 1 - MISC results for P(MISC > 5) (left) and P(MISC>9) (right) for different population motion sickness susceptibilities.

Moreover, Figure 4 indicates that the bow is predicted to cause the highest levels of motion sickness, consistent with the elevated power observed in Figure 3. The higher intensity of accelerations in this region affects the experienced motion sickness. Conversely, the lowest perceived motion sickness is predicted for the position closest to the vessel's center of mass, which is typically close to the center of rotation. At that point, the tangential and centripetal accelerations are the least compared to other positions on the vessel.

Variations in the population's sensitivity to motion sickness are illustrated in Figure 5. The percentiles in the figure represent the portion of the population most resistant to motion sickness.

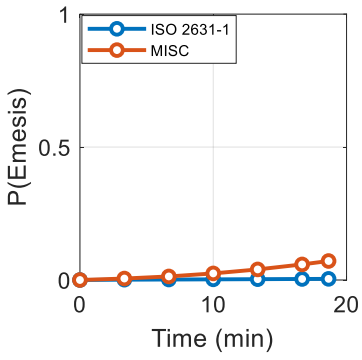

Figure 6. Scenario 1 - MISC results for P(MISC>9) compared with ISO 2631-1 at crew location.

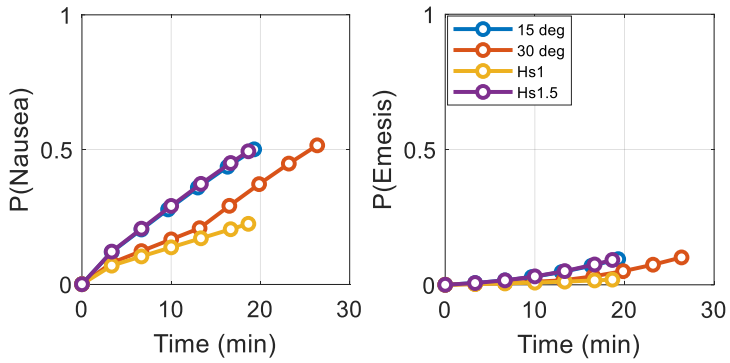

Figure 7. Scenario 1 - MISC results at the crew location for a 15 degree deviation, a 30 degree deviation, Hs=1, and Hs=1.5.

For example, the 10th percentile corresponds to the 10% of the population with the highest resistance. The results highlight significant individual differences in perceived motion sickness.

Figure 6 highlights the differences between the ISO 2631-1 and the MISC-based model, revealing a discrepancy in perceived motion sickness, with the MISC-based model typically predicting higher levels. These higher levels are largely explained by the fact that the pre-emesis symptoms reckoned by the MISC-based model result in a wider frequency weighting function, in particular at the higher frequencies. Another reason is that the MISC-based model accounts for motion in the *x*-, *y*-, and *z*-directions. In particular, the observed *y*-direction shows significantly more power at frequencies above 1 Hz that do contribute to pre-emesis symptoms, whereas the ISO 2631-1 model considers only the z-direction which frequency weighting typically only shows marginal effects on emesis above 1 Hz.

Another potential limitation is the MISC-based model's limited validation for accelerations exceeding 4 m/s ^{2}. Since the model has been primarily tested and validated for the lower accelerations common in land-based vehicles, its accuracy at higher accelerations remains uncertain. This raises the possibility that the model may not be well-suited for such conditions, which could result in inaccurate predictions. Similarly, the predicted vessel motions should undergo validation to confirm their accuracy. A more comprehensive study is important to thoroughly assess the model's performance across a broader range of accelerations.

Figure 7 illustrates the effects of a calmer sea state on scenario 1. The MISC-based model predictions for a significant wave height (Hs) of 1 meter are shown to be more than halved by the end of the trip compared to the predictions for a sea state with a Hs of 1.5 meters, as depicted in Figure 3. This reduction in predicted motion sickness is expected because the total power of the vessel's motions increases in rougher seas with higher waves, while the trip duration remains constant.

The interaction between waves and vessels is a complex phenomenon, with deviations in the angle of incoming waves significantly influencing vessel motions. To explore whether modifying the transit path could reduce motion sickness, an alternative to sailing in a straight line was tested. This approach involves splitting the journey into two equal-length segments, where the angle of deviation from the straight path determines their lengths. Practically, this deviation can be to the left or right of the straight line, but for modeling purposes, a constant sea state is assumed, making left and right deviations effectively identical as the deviated paths are parallel to each other. Figure 7 presents the results for deviation angles of 15° and 30°. Since a straight line represents the shortest Euclidean distance, deviations result in a longer path and thus increased travel time. As

expected due to the geometries of the paths, smaller deviation angles lead to marginally longer travel times, while larger angles have more significant effects on travel time. Although deviations to the straight line reduce the intensity of vessel motions by altering wave interactions, the extended exposure duration to these lesser motions offsets the benefits.

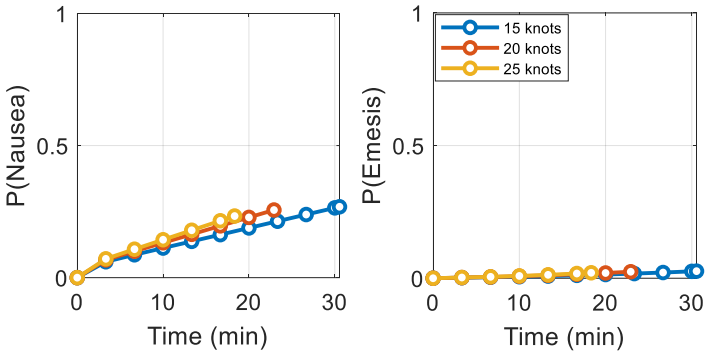

Figure 8. Scenario 2 - MISC results for 15, 20, and 25 knots.

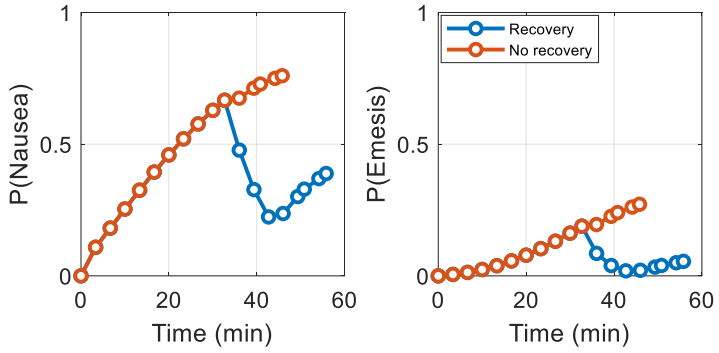

Figure 9. Scenario 3 - MISC results for rest after segment 1.

In this implementation, the initial deviation angle and the angle used to turn back toward the endpoint are identical, creating two equal-length segments. While experiments have varied the deviation angle, altering the relative lengths of these segments has not been investigated in this study. Future research could focus on optimizing the deviation route by adjusting both the angles and the lengths of each segment, potentially enhancing the effectiveness of alternative routes.

Scenario 2

The accuracy of the MISC-based model depends on the reliability of the hydrodynamic model, which in turn relies on a suitable RAO dataset. To minimize the rounding effects inherent in lower-speed scenarios, an arbitrary route is chosen for Scenario 2, ensuring wave angles align with RAO resolution steps.

The results for this scenario are shown in Figure 8. Lowering the speed from 25 knots to 20 knots or 15 knots increases the predicted motion sickness by the end of the trip. While the motion sickness increases more slowly over time at lower speeds, the longer trip duration compensates for the smaller rate of increase, resulting in worse outcomes for slower transit speeds. Similar to the deviated route, reducing the vessel's speed leads to a decrease in the speed at which motion sickness accumulates over time. However, this also increases the total travel time, resulting in a trade-off between reduced motion sickness per unit of travel time and the overall duration of the trip.

Scenario 3

A scenario in which technicians rest at a given wind turbine is analyzed, assuming the rest occurs in a nearly motionless environment, such as the transition piece or inside the wind turbine tower. In this scenario, the CTV transports four technician teams to four different turbines (Figure 2), with the rest period occurring at the first turbine. The analysis, shown in Figure 9, predicts that a 10-minute break at the first turbine reduces motion sickness over time considerably. Although motion sickness increases again once the CTV resumes transit to subsequent turbines, the rest period does result in significant lower levels of sickness at the end. In practice, time would be

required for technician teams to disembark and reach the transition piece, and the vessel's deceleration and hovering near the turbine would generate motion patterns distinct from the constant motion at 25 knots. These factors, not accounted for in this study, could further influence the predictions.

4. Conclusion

This study lays the foundation for integrating the MISC-based motion sickness model into daily O&M scheduling tools for offshore wind applications. The model uses vessel motion data to estimate motion sickness based on accelerations, predicting a range of symptoms on the MISC scale. Standalone scenarios were evaluated to showcase potential applications, including analyses of motion sickness in different vessel locations, susceptibilities, weather conditions, vessel velocities, routes, and breaks. Significant effects on motion sickness were observed with reduced wave heights and breaks, while reduced vessel velocity and deviating routes did not improve motion sickness due to increased transit time.

In conclusion, while the MISC-based motion sickness model presented in this study has not yet been validated for marine applications, the primary objective was to demonstrate its potential use in offshore wind O&M planning. The findings demonstrate how incorporating motion sickness predictions into decision-making processes can provide value by enabling more informed planning strategies. From a managerial perspective, this allows better resource allocation because the risk of technician downtime and aborted missions due to health-related issues is reduced. Furthermore, a crew that has suffered less motion sickness will be more effective, therefore increasing both safety and productivity. Finally, motion sickness predictions can help guide decision-making for investments in vessel types or onboard mitigation measures (e.g., stabilization systems).

Future research should focus on validating the model specifically for marine environments, optimizing its integration into daily O&M planning tools such as Despatch, and quantifying the impact of motion sickness on technician performance. Additionally, validating and refining the vessel motion model should be considered to ensure that its predictions accurately represent real-world conditions.

Bibliography

[1] IRENA, "Wind Energy," 11 06 2024. [Online]. [Accessed 2024].

[2] J. Bos, "How motions make people sick such that they perform less: a model based approach," in *NATO RTO/AVT-110 Symp. Habitability of Combat and Transport Vehicles: Noise, Vibration and Motion*, Prague, 2004.

[3] A. Stormonth-Darling, "SPOWTT Final Project Report," European Union's Horizon 2020 research and innovation programme, 2020.

[4] F. Earle, J. Huddlestone, T. Williams, C. Stock-Williams, H. van der Mijle-Meijer, L. de Vries, H. van Heemst, E. Hoogerwerf, L. Koomen, E.-J. de Ridder, J.-J. Serraris, G. Struijk, A. Stormonth-Darling, J. Cline, M. Jenkins, J. G. dos Santos, I. Coates, A. Corrie and G. Moore,

"SPOWTT: Improving the safety and productivity of offshore wind technician transit," *Wind Energy,* vol. 25, p. 34–51, 2020.

[5] C. Stock-Williams and S. K. Swamy, "Automated daily maintenance planning for offshore wind farms," *Renewable Energy,* vol. 133, pp. 1393-1403, 2019.

[6] P. D. Tomaselli, M. Dixen, R. Bolaños Sanchez and J. Tirnfeldt Sørensen, "A Decision-Making Tool for Planning O&M Activities of Offshore Wind Farms Using Simulated Actual Decision Drivers," *Marine Science,* p. 7:588624, 2021.

[7] B. Hu, S. Swamy and K. Hermans, "Including Realistic Vessel and Human Behaviour in Simulations of Offshore Wind Farm Operations," TNO, Petten, 2018.

[8] MARIN, "Offshore maintenance JIP II," MARIN, 2020.

[9] "TNO UWiSE," TNO, [Online]. Available: https://uwise.tno.nl/. [Accessed 03 12 2024].

[10] J. Journée and W. Massie, Offshore Hydromechanics, Delft: Delft University of Technology, 2001.

[11] S. Alexander, M. Cotzin, C. Hill, E. Ricciuti Jr. and G. Wendt, "Wesleyan University Studies of Motion Sickness: III. The Effects of Various Accelerations Upon Sickness Rates," *The Journal of Psychology,* vol. 20, no. 1, pp. 3-8, 1945.

[12] S. Alexander, M. Cotzin, C. Hill, C. Hill and G. Wendt, "Wesleyan University Studies of Motion Sickness: IV. The Effects of Waves Containing two Acceleration Levels Upon Sickness," *The Journal of Psychology,* vol. 20, no. 1, pp. 9-18, 1945.

[13] J. F. Golding, H. Markey and J. Stott, "The effects of motion direction, body axis, and posture on motion sickness induced by low frequency linear acceleration," *Aviation, Space, and Environmental Medicine,* vol. 66, no. 11, pp. 1046-1051, 1995.

[14] M. J. Griffin and K. L. Mills, "Effect of Frequency and Direction of Horizontal Oscillation on Motion Sickness," *Aviation, Space, and Environmental Medicine,* vol. 73, pp. 537-543, 2002.

[15] M. J. Griffin and K. L. Mills, "Effect of Magnitude and Direction of Horizontal Oscillation on Motion Sickness," *Aviation, Space, and Environmental Medicine,* vol. 73, pp. 640-646, 2002.

[16] J. E. Bos, S. N. MacKinnon and A. Patterson, "Motion Sickness Symptoms in a Ship Motion Simulator: Effects of Inside, Outside, and No View," *Aviation, Space and Environmental Medicine,* vol. 76, no. 12, pp. 1111-1118, 2005.

[17] A. Reuten, S. Nooij, J. Bos and J. Smeets, "How feelings of unpleasantness develop during the progression of motion sickness symptoms," *Experimental Brain Research,* vol. 239, no. 12, pp. 3615-3624, 2021.